All-Electrical Measurement of the Density of States in (Ga,Mn)As

D. Neumaier,* M. Turek,† U. Wurstbauer,‡ A. Vogl, M. Utz, W. Wegscheider,§ and D. Weiss

Institut für Experimentelle und Angewandte Physik, University of Regensburg, Germany

(Received 16 February 2009; published 19 August 2009)

We report on electrical measurements of the effective density of states in the ferromagnetic semiconductor material (Ga,Mn)As. By analyzing the conductivity correction to an enhanced electron-electron interaction the electrical diffusion constant was extracted for (Ga,Mn)As samples of different dimensionality. Using the Einstein relation allows us to deduce the effective density of states of (Ga,Mn)As at the Fermi energy.

DOI: 10.1103/PhysRevLett.103.087203 PACS numbers: 75.50.Pp, 71.20.−b, 73.23.−b

The ferromagnetic semiconductor (Ga,Mn)As [1] has been studied intensely over the last decade and has become a model system for future spintronics applications [2,3]. With typical Mn concentrations between 1% and 15% maximum Curie temperatures of up to ~180 K have been reported [4,5]. Mn atoms on Ga-sites provide both holes and magnetic moments. For Mn concentrations larger than 1%, the impurity wave functions at the Fermi energy overlap and a metallic state forms. The ferromagnetic order between the magnetic moments of the Mn ions is mediated by the delocalized holes [6]. A topic of current debate is whether the holes reside in an impurity band, detached and above the valence band, or in the valence band [7–10]. A mean-field picture based on the latter scenario allowed to predict, e.g., Curie temperature [6] or magnetocrystalline anisotropies [11] in (Ga,Mn)As correctly. On the other hand, optical absorption experiments, carried out, e.g., in Ref. [12,13], suggest that even for high manganese concentrations of up to 7% the Fermi energy stays in an impurity band, detached from the valence band, with a high effective hole mass m^* of order ten free electron masses m_e [12]. An analysis of the mobility in (Ga,Mn)As with hole concentration above $1 \times 10^{26}/\mathrm{m}^3$ also suggests $m^* \sim 30 m_e$ [14]. However, there is also indication that the impurity band and the valence band have completely merged as discussed in Ref. [7] and references therein. In the present Letter, we make use of the well-known quantum mechanical conductivity correction due to electron-electron interaction (EEI) to extract the diffusion constant and hence the density of states at the Fermi energy, $N(E_F)$. The electrically measured values of $N(E_F)$ will be compared with recent theoretical calculations.

In ferromagnetic (Ga,Mn)As, the conductivity is decreasing with decreasing temperature below 10 K. This conductivity decrease can be explained by enhanced electron-electron interaction [15]. The effect of EEI arises from a modified screening of the Coulomb potential due to the carriers' diffusive motion and depends on the dimensionality of the conductor [16]. As the conductivity decrease due to enhanced electron-electron interaction is depending on the electrical diffusion constant D, a detailed analysis of the conductivity decrease, different for different dimensionality, provides experimental access to the diffusion constant. Using the Einstein relation $\sigma = N(E_F)De^2$, with the conductivity σ, the effective density of states at Fermi's energy, $N(E_F)$, can be determined.

To investigate electron-electron interaction in quasi 1D, 2D and 3D systems we fabricated Hall-bar mesas (2D and 3D) and wire arrays (1D and crossover regime from 1D to 2D) out of several wafers, having a $(Ga_{1-x}, Mn_x)As$ layer on top of semi-insulating GaAs [17]. The nominal Mn concentration x was approx. 4% (sample 1_{3D} and 2_{3D}) and ~6% (other samples). The relevant parameters of the samples are listed in Table I. The dimensionality for EEI is defined by the number of spatial dimensions larger than the thermal diffusion length $L_T = \sqrt{\hbar D/k_B T}$. In (Ga,Mn)As $L_T \approx 120$–200 nm at 20 mK, depending on the exact value of the diffusion constant D. Hence, the thick Hall-bar mesas (150 and 300 nm) can be considered as quasi 3D,

TABLE I. Length l, width w, thickness t and number of lines parallel N of the samples. We used the sheet resistance at room temperature and the lengths of the wires to determine the average electrically active width of the wires, denoted as width. The geometric width, read off the electron micrographs, is typically ~4 nm wider. Curie temperature T_C and carrier concentration p were taken on reference samples from the corresponding wafers. p was measured using the Hall effect as described in Ref. [18]. Annealed samples are marked by "A."

Sample	l (μm)	w (μm)	t (nm)	N	T_C (K)	p ($10^{26}/\mathrm{m}^3$)
1_{1D}	7.5	0.042	42	25	90	3.8
$1_{1D}A$	7.5	0.042	42	25	150	9.3
2_{1D}	7.5	0.035	42	12	90	3.8
$1_{1D-2D}A$	10	0.067	30	25	150	8.6
$2_{1D-2D}A$	10	0.092	30	25	150	8.6
$3_{1D-2D}A$	10	0.170	30	25	150	8.6
$4_{1D-2D}A$	10	0.242	30	25	150	8.6
1_{2D}	180	11	42	1	90	3.8
1_{3D}	240	10	150	1	?	1.4
2_{3D}	240	10	300	1	75	2.1

while the thin Hall-bar mesa (42 nm) is quasi 2D, at least below ~500 mK. The smallest wires (42 and 35 nm) behave quasi 1D and the wider wires (67 to 242 nm) are in the crossover regime from 1D to 2D, as is shown below. Arrays of wires with N wires in parallel were fabricated to suppress universal conductance fluctuations by ensemble averaging. The Hall bars were fabricated using optical lithography and wet chemical etching. For fabricating the wire arrays, we used electron-beam lithography and chemical dry etching. The contact pads to the devices were made by thermal evaporation of Au and liftoff. The measurements of the conductivity were performed in a top-loading dilution refrigerator using standard four-probe lock-in technique. To suppress conductivity contributions due to weak localization, we applied a perpendicular magnetic field of $B = 3$ T. At $B = 3$ T no weak localization can be observed in (Ga,Mn)As [19,20] even at 20 mK.

According to Lee and Ramakrishnan [16], the temperature dependency of the conductivity correction due to EEI is depending on the dimensionality of the sample with respect to L_T. For 1D systems, the expected temperature dependency is $\propto -1/\sqrt{T}$, for 2D $\propto \log_{10}(T/T_0)$ and for 3D $\propto\sqrt{T}$. Corresponding data for 1D, 2D, and 3D (Ga,Mn)As-samples, shown in Figs. 1(b)–1(d) confirm the expected temperature dependency below 1 K. Hence, the decreasing conductance with decreasing temperature in (Ga,Mn)As can be attributed to EEI.

The size of the conductivity correction due to electron-electron interaction is depending on the diffusion constant D in 1D systems [16]:

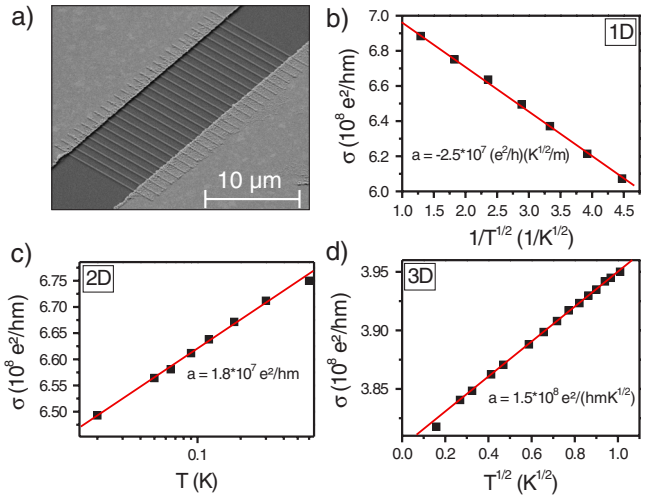

FIG. 1 (color online). (a) Electron micrograph of a line array having 25 lines in parallel (Sample $2_{1D-2D}A$). The width of the lines is 92 nm, the length is 10 μm. (b), (c), and (d) Conductivity of the quasi 1D line array 1_{1D} (b), the quasi 2D Hall-bar 1_{2D} (c) and the quasi 3D Hall-bar 2_{3D} (d) plotted versus temperature. The straight lines are guide for the eyes. The slope of the lines are given.

$$\Delta\sigma = -\frac{F^{1D}}{\pi w t}\frac{e^2}{\hbar}\sqrt{\frac{\hbar D}{k_B T}}, \tag{1}$$

and also in 3D systems [16]:

$$\Delta\sigma = \frac{F^{3D}}{4\pi^2}\frac{e^2}{\hbar}\sqrt{\frac{k_B T}{\hbar D}}. \tag{2}$$

As the conductivity correction due to EEI is also depending on the screening parameters $F^{1D,2D,3D}$, one needs to know the corresponding parameter to extract D from the conductivity correction. Only in quasi 2D systems the conductivity correction is independent on the diffusion constant [16]:

$$\Delta\sigma = \frac{F^{2D}}{2t\pi^2}\frac{e^2}{\hbar}\log\frac{T}{T_0}. \tag{3}$$

Hence, in the 2D case, F^{2D} can be directly extracted from experiment. As already shown in previous work [15], the screening parameter F^{2D} in (Ga,Mn)As ranges from 1.8 to 2.6 and is in excellent agreement with the screening parameter in Co, Co/Pt-multilayers, and Permalloy. In these ferromagnetic metals, F^{2D} is between 2.0 and 2.6 [21–23]. Thus, using the well-known parameters F^{1D} of other ferromagnetic metals is a good approximation for F^{1D} in (Ga,Mn)As. In Ni and Py nanowires, F^{1D} is 0.83 and 0.77, respectively [23,24]. Consequently, $F^{1D} = 0.80 \pm 0.12$ should be a good approximation for the screening parameter of quasi 1D (Ga,Mn)As samples. With this F^{1D} parameter, we can calculate the diffusion constant of sample 1_{1D} using Eq. (1): $D = 10 \pm 3 \times 10^{-5}$ m^2/s. Using the Einstein relation, this value corresponds to an effective density of states $N(E_F) = 1.1 \pm 0.3 \times 10^{46}/\mathrm{J\,m^3}$ at the Fermi energy.

It is more difficult to estimate the value of F^{3D} as no data are available for 3D ferromagnetic metals. Therefore, we have to rely on theoretical predictions for the screening parameter: $F^{3D} = 1.2$ [25]. Though the calculations of the 2D screening parameter ($F^{2D} = 2.3$ [25]) agree well with the experimental values of different ferromagnets ($F^{2D} = 1.8, \ldots, 2.6$), they are less accurate for 1D systems. For 1D systems, F^{1D} was calculated to be 1.6, while the typical experimental values of $F^{1D} \approx 0.8$ are by a factor of 2 smaller [23,24]. Hence, by using the theoretical value for F^{3D}, we need to take into account an uncertainty of order 100%. Using Eq. (2) and the theoretical value for $F^{3D} = 1.2$ [25], we arrive at $D = 2.2 \times 10^{-5}$ m^2/s for sample 2_{3D}. Using the Einstein relation this corresponds to $N(E_F) = 2.0 \times 10^{46}/\mathrm{J\,m^3}$, with a high uncertainty of approx. 200%.

The different temperature dependence of EEI in 1D ($\Delta\sigma \propto -1/\sqrt{T}$) and 2D ($\Delta\sigma \propto \ln T$) together with the temperature dependence of the thermal length $L_T = \sqrt{\hbar D/k_B T}$ allows to use another scheme to extract the diffusion constant and hence $N(E_F)$. By measuring the

dimensional crossover, i.e., the change of the temperature dependence of the conductivity correction as a function of the sample size, one can fit both, diffusion constant and screening parameter independently. We thus do not have to rely on literature values of F^{1D}. Here, we used the crossover from 1D to 2D to determine D. For this experiment, wire arrays with wire widths, ranging from 67 to 242 nm (sample $1_{1D-2D}A, \ldots, 4_{1D-2D}A$ in Table I), were patterned on the same wafer. These four wires are in the crossover regime between 1D and 2D. In the crossover regime, the conductivity correction due to EEI is given by an interpolation formula [26]:

$$\Delta\sigma t = -F\frac{e^2}{\pi\hbar}\sum_{n=0}^{\infty}\left[\frac{w^2}{L_T^2}+(n\pi)^2\right]^{-1/2}-\left[\frac{w^2}{L_{T_0}^2}+(n\pi)^2\right]^{-1/2}, \quad (4)$$

with one screening parameter F and T_0, the lowest temperature. Figure 2(a) shows the conductivity change from 1 K to 22 mK of all four wire arrays. The conductivity change increases markedly with decreasing wire width. To extract the characteristic parameters, we fitted the data using Eq. (4) with D and F as free parameters. The diffusion constant affects essentially the width dependence (x scale) while the screening parameter F shifts the curve on the y scale. Hence, the fit is unique and allows to extract D and F independently. The best fitting result was obtained by using $D = 9 \times 10^{-5}$ m^2/s and $F = 1.08$ (middle line). To illustrate the sensitivity of the fitting procedure on D, we also plotted Eq. (4) using $D = 12 \times 10^{-5}$ m^2/s and $D = 6 \times 10^{-5}$ m^2/s. Here, F was the free parameter to optimize the fit. Both traces describe the experimental data less satisfying than the red trace. Hence, the measurement of the dimensional crossover from 1D to 2D results in $D = 9 \pm 1.5 \times 10^{-5}$ m^2/s. In Fig. 2(b), the conductivity change with respect to 22 mK is plotted for all four wire arrays (sample $1_{1D-2D}A$ to $4_{1D-2D}A$) versus temperature. The lines are the calculated conductivity correction given by Eq. (4). The parameters used are $D = 9 \times 10^{-5}$ m^2/s and $F = 1.08$. The conductivity correction in the whole temperature range from 22 mK to 1 K of all four wire arrays is perfectly described by using only these two parameters D and F. Also in the crossover regime from 1D to 2D, the observed screening parameter $F = 1.08$ is in excellent agreement with the screening parameter observed in Co ($F = 0.95$) [21]. From the obtained diffusion constant, we can estimate the effective density of states using the Einstein relation: $N(E_F) = 1.6 \pm 0.3 \times 10^{46}$/J m^3.

To check the consistency of both presented methods, we can also treat the four samples ($1_{1D-2D}A$ to $4_{1D-2D}A$) as quasi 1D at low temperatures (indicated by the straight lines in the inset of Fig. 2(a)] and calculate the diffusion constant using Eq. (1) and $F^{1D} = 0.8$ as described above. When doing so, we obtain $D = 8.4 \pm 2.5 \times 10^{-5}$ m^2/s. This is in good agreement with the value estimated by fitting the crossover from 1D to 2D, and hence the two methods are consistent.

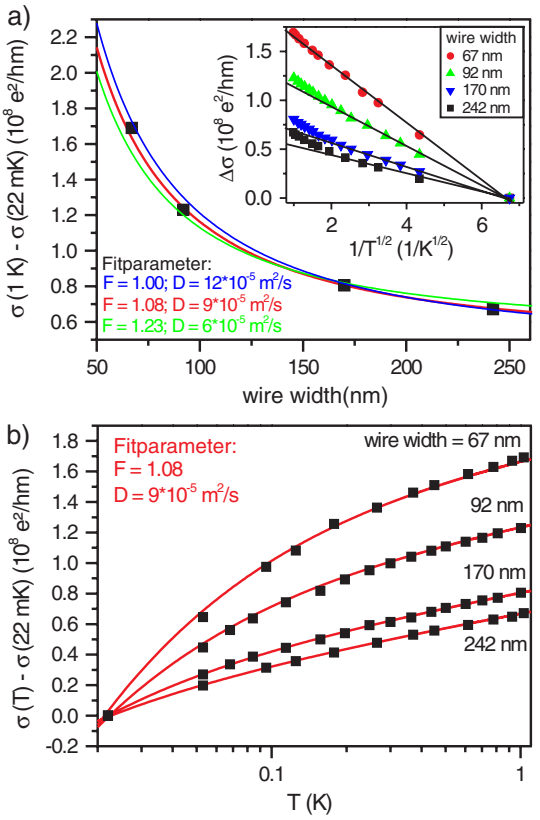

FIG. 2 (color online). (a) Conductivity change from 1 K to 22 mK of four line arrays (sample $1_{1D-2D}A, \ldots, 4_{1D-2D}A$) plotted versus the wire width. The middle line is the best fit of the data to Eq. (4). The other two lines are fits using Eq. (4) and a diffusion constant of 12×10^{-5} m^2/s and 6×10^{-5} m^2/s, respectively. In the inset, the conductivity change of four wire arrays (sample $1_{1D-2D}A, \ldots, 4_{1D-2D}A$) is plotted versus $1/\sqrt{T}$. The slopes are guide for the eyes. (b) Conductivity change of the four line arrays (sample $1_{1D-2D}A, \ldots, 4_{1D-2D}A$) plotted versus temperature. The lines are calculated using Eq. (4) and the parameters obtained by fitting the data in (a).

Figure 3 summarizes our findings and shows the extracted effective density of states versus the carrier concentration (circles). The data are compared to calculations based on four different models: The upper line describes a parabolic, fully spin polarized and nondegenerated band with high effective mass of $30m_e$ as an approximation for a detached impurity band. The grey line stems from a 6×6 $k \cdot p$ model with parameters for the GaAs valence band, calculated by T. Dietl *et al.* and based on Ref. [27]. The corresponding effective hole mass is $\sim 1m_e$ in the investigated range of carrier concentration. In addition, we performed numerical simulations which are based on a multiband tight-binding approach applied to disordered bulk systems using two different parameter sets. The first model was derived from first principles calculations for (Ga,Mn)As [28] (model Masek). The second one describes

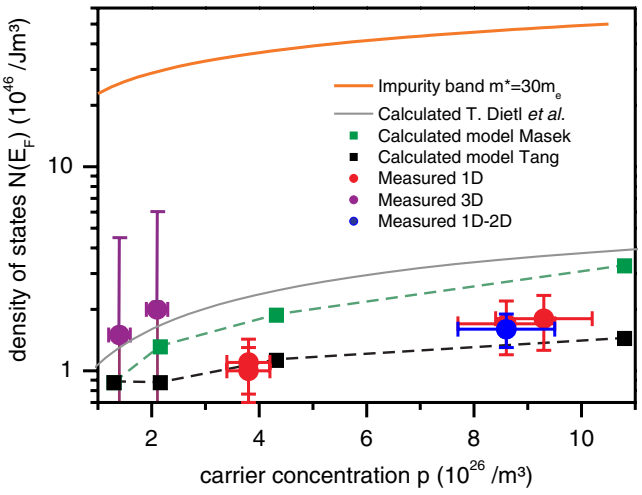

FIG. 3 (color online). Density of states at Fermi's energy plotted versus carrier concentrations. The squares are calculated using the model of Masek *et al.* and the model of Tang and Flattè, respectively. The upper line describes a parabolic, fully spin polarized and nondegenerated band with high effective mass of $30m_e$ as an approximation for a detached impurity band. The grey line gives $N(E_F)$ calculated using a 6×6 $k \cdot p$ model with parameters for the GaAs valence band [27]. The circles are measured using EEI in 1D, 3D, and in the crossover regime from 1D to 2D.

the Mn impurities by a modified on-site potential and a spin-dependent potential at the four nearest neighbor As sites which reproduce the experimental binding energy of 113 meV [29] (model Tang). A detailed description of the method and the two models is given in Ref. [30]. Neither model exhibits a detached impurity band for Mn concentrations larger than 1%. The effective masses were estimated to lie in the range $m^* = 0.4, \ldots, 0.6m_e$ for the considered carrier concentrations with only minor quantitative differences between the two models. The experimental data appear to favor the Tang and Flattè model, while uncertainties in the hole compensation level by Mn interstitials do not allow us to make conclusive remarks as to which model is more realistic. Only the case of a detached impurity band with high effective mass can be ruled out, as it would lead to an effective density of states more than one order above the measured values.

In conclusion, we have demonstrated that the effective density of states at the Fermi energy of (Ga,Mn)As can be extracted from conductivity measurements, i.e., an analysis of the conductivity correction due to EEI. The measured values of $N(E_F)$ are consistent with a picture that the Fermi energy is located within the GaAs valence band or an impurity band, merged with the valence band. Our experimental finding with effective masses of $\sim 1m_e$ is however at odds with a detached impurity band, where the effective hole mass is much larger than m_e.

We thank T. Dietl and J. Fabian for stimulating discussions and the Deutsche Forschungsgemeinschaft (DFG) for their financial support via SFB 689.

*neumaier@amo.de; Present address: AMO GmbH, Aachen, Germany
†Present address: Fraunhofer CSP, Halle, Germany
‡Present address: Institut für Angewandte Physik, University of Hamburg, Germany
§Present address: Solid State Physics Laboratory, ETH Zurich, 8093 Zurich, Switzerland

[1] H. Ohno, Science **281**, 951 (1998).
[2] I. Žutić, J. Fabian, and S. Das Sarma, Rev. Mod. Phys. **76**, 323 (2004).
[3] J. Fabian *et al.*, Acta Phys. Slovaca **57**, 565 (2007).
[4] K. Olejník *et al.*, Phys. Rev. B **78**, 054403 (2008).
[5] M. Wang *et al.*, Appl. Phys. Lett. **93**, 132103 (2008).
[6] T. Dietl *et al.*, Science **287**, 1019 (2000).
[7] T. Jungwirth *et al.*, Phys. Rev. B **76**, 125206 (2007).
[8] T. Jungwirth *et al.*, Rev. Mod. Phys. **78**, 809 (2006).
[9] K. S. Burch, D. D. Awschalom, and D. N. Basov, J. Magn. Magn. Mater. **320**, 3207 (2008).
[10] A. H. MacDonald, P. Schiffer, and N. Samarth, Nature Mater. **4**, 195 (2005).
[11] M. Sawicki, J. Magn. Magn. Mater. **300**, 1 (2006), and references therein.
[12] K. S. Burch *et al.*, Phys. Rev. Lett. **97**, 087208 (2006).
[13] K. Ando *et al.*, Phys. Rev. Lett. **100**, 067204 (2008).
[14] K. Alberi *et al.*, Phys. Rev. B **78**, 075201 (2008).
[15] D. Neumaier *et al.*, Phys. Rev. B **77**, 041306(R) (2008).
[16] P. A. Lee and T. V. Ramakrishnan, Rev. Mod. Phys. **57**, 287 (1985).
[17] M. Reinwald *et al.*, J. Cryst. Growth **278**, 690 (2005).
[18] K. W. Edmonds *et al.*, J. Appl. Phys. **93**, 6787 (2003).
[19] D. Neumaier *et al.*, Phys. Rev. Lett. **99**, 116803 (2007).
[20] L. P. Rokhinson *et al.*, Phys. Rev. B **76**, 161201(R) (2007).
[21] M. Brands *et al.*, Phys. Rev. B **74**, 033406 (2006).
[22] M. Brands, A. Carl, and G. Dumpich, Ann. Phys. (Leipzig) **14**, 745 (2005).
[23] D. Neumaier *et al.*, Phys. Rev. B **78**, 174424 (2008).
[24] T. Ono *et al.*, J. Magn. Magn. Mater. **226**, 1831 (2001).
[25] R. Raimondi, P. Schwab, and C. Castellani, Phys. Rev. B **60**, 5818 (1999).
[26] G. Neuttiens *et al.*, Europhys. Lett. **34**, 617 (1996).
[27] T. Dietl, H. Ohno, and F. Matsukura, Phys. Rev. B **63**, 195205 (2001).
[28] J. Masek *et al.*, Phys. Rev. B **75**, 045202 (2007).
[29] J.-M. Tang and M. E. Flattè, Phys. Rev. Lett. **92**, 047201 (2004).
[30] M. Turek, J. Siewert, and J. Fabian, Phys. Rev. B **78**, 085211 (2008).